Aperiodic stochastic resonance

J. J. Collins,[1,2] Carson C. Chow,[1] Ann C. Capela,[1,2] and Thomas T. Imhoff[1]
[1]*NeuroMuscular Research Center, Boston University, 44 Cummington Street, Boston, Massachusetts 02215*
[2]*Department of Biomedical Engineering, Boston University, 44 Cummington Street, Boston, Massachusetts 02215*
(Received 17 June 1996)

Stochastic resonance (SR) is a phenomenon wherein the response of a nonlinear system to a weak periodic input signal is optimized by the presence of a particular level of noise. Recently, we presented a method and theory for characterizing SR-type behavior in excitable systems with aperiodic (i.e., broadband) input signals [Phys. Rev. E **52**, R3321(1995)]. We coined the term *aperiodic stochastic resonance* (ASR) to describe this general type of behavior. In that earlier study, we demonstrated ASR in the FitzHugh-Nagumo neuronal model. Here we demonstrate ASR in three additional systems: a bistable-well system, an integrate-and-fire neuronal model, and the Hodgkin-Huxley (HH) neuronal model. We present computational and theoretical results for each system. In the context of the HH model, we develop a general theory for ASR in excitable membranes. This work clearly shows that SR-type behavior is not limited to systems with periodic inputs. Thus, in general, noise can serve to enhance the response of a nonlinear system to a weak input signal, regardless of whether the signal is periodic or aperiodic. [S1063-651X(96)02611-6]

PACS number(s): 87.22.Jb, 05.40.+j

I. INTRODUCTION

Stochastic resonance (SR) is a phenomenon in which the response of a nonlinear system to a weak periodic input signal is optimized by the presence of a particular level of noise [1]. The notion of SR was originally proposed as a possible explanation for periodic recurrences in global climate dynamics [2]. Since then, SR has been examined experimentally in a wide variety of systems, including electronic systems [3], optical systems [4], magnetic systems [5,6], mechanical systems [7], and biological systems [8–10]. Moreover, theories of SR have been developed for multistable [11] and excitable [12] systems, as well as threshold-crossing detectors [13]. These developments have pointed to the possible beneficial effects of noise on the dynamics of nonlinear systems. It is important to note, however, that all of the aforementioned work has been restricted to systems with periodic inputs. This focus has served to limit the applicability of SR to practical situations, given that real-world external signals are typically not periodic.

Recently, we developed a method for characterizing SR-type behavior in excitable systems with aperiodic (arbitrary) inputs [14] that emphasizes the ''shape matching'' between the input and output signals. For this general type of behavior, we coined the term *aperiodic stochastic resonance* (ASR). We have demonstrated ASR computationally in the FitzHugh-Nagumo (FHN) neuronal model [14] and in a summing network of FHN model neurons [15]. We have also developed a theory to account for these results [14,15]. More recently, we have demonstrated ASR experimentally in rat cutaneous sensory neurons [16]. These developments [17] indicate that noise can serve to enhance the response of a nonlinear system to a weak input signal, regardless of whether the signal is periodic or aperiodic. In this paper, we extend our work on ASR to three additional systems: a bistable-well system, an integrate-and-fire neuronal model, and the Hodgkin-Huxley (HH) neuronal model. Previous studies have considered bistable-well systems with nonperiodic input signals [18,19]. However, in contrast with the present work and our earlier ASR studies [14–16], these investigations [18,19] concentrated on distorted harmonic signals and used single-frequency measures to characterize SR.

This paper is organized as follows. In Sec. II, we describe the measures used to characterize ASR. In Secs. III and IV, we present computational and theoretical results for a bistable-well system and an integrate-and-fire neuronal model, respectively. In Sec. V, we present numerical results for the HH model and a general theory for ASR in excitable membranes. We show that the theory is applicable to both the FHN model and the HH model. Finally, in Sec. VI, we discuss the implications of the presented results and describe possible technological and bioengineering applications of ASR.

II. ASR MEASURES

In general, the phenomenon of SR indicates that the flow of information through a system (i.e., the coherence between the input stimulus and the system response) is optimized by the presence of a particular level of noise [1,20–22]. In line with this operational definition, SR has typically been characterized by examining the output signal-to-noise ratio, which is computed from the power spectrum and defined as the ratio of the strength of the signal peak (i.e., its area) to the mean amplitude of the background noise at the input signal frequency [9,12,20]. In excitable systems, SR has also been characterized by examining the modes in the interspike interval histograms [23] located at integer multiples of the input signal period [8,9,24]. Both of these methods assess the coherence of the response of the system with the input signal frequency. Thus these techniques are clearly inappropriate for systems with aperiodic inputs.

In Ref. [14], we proposed two cross-correlation measures for characterizing ASR: the power norm and the normalized power norm. We used these measures to characterize ASR in the FHN model [14]. Here we demonstrate the generality of

these measures for any system that can make transitions between different states. We characterize the system's response to an arbitrary input signal plus Gaussian white noise as the mean transition rate (averaged over a time window) between these states.

The power norm C_0 is defined as

$$C_0 = \max\{\overline{S(t)R(t+\tau)}\}, \tag{1}$$

where $S(t)$ is the aperiodic (zero-mean) input signal, $R(t)$ is the response of the system characterized by the mean transition rate, τ is a time lag, and the overbar denotes an average over time. [For ASR, the exact form of $S(t)$ is unimportant, provided its variations occur on a time scale that is slower than the characteristic time(s) of the system under study.] Note that C_0 is a scalar measure that quantifies the maximum in the input-output cross-correlation function which is a function of the time lag τ.

The normalized power norm C_1 (or cross-correlation coefficient) is defined as

$$C_1 = \frac{C_0}{[\overline{S^2(t)}]^{1/2}\{\overline{[R(t)-\overline{R(t)}]^2}\}^{1/2}}. \tag{2}$$

From a signal-processing perspective, maximizing C_1 corresponds to maximizing the shape matching between the input stimulus $S(t)$ and the system response $R(t)$, whereas maximizing C_0 corresponds to taking account of both signal amplification and shape matching. These measures thus enable one to quantify the two noise-induced effects associated with SR, i.e., the original notion of signal amplification [2] and the later notion of optimal stimulus-response coherence [1,4,20–22].

More recently, information-theoretic measures (e.g., transinformation) have been used to characterize SR and ASR in model neurons [25,26] and the cricket cercal sensory system [27]. These measures will not be considered here. However, it is worth noting that in an ASR study with the FHN model [26], it was shown that a peak in the cross-correlation measures C_0 and C_1, respectively, for a particular level of input noise is matched by a peak in the transinformation. Thus, for cases with subthreshold aperiodic input stimuli, the addition of noise can optimize the information-transfer rate, as well as second-order coherence measures.

III. BISTABLE-WELL SYSTEM

We first consider a symmetric bistable-well system with a fluctuating barrier, as given by

$$\frac{dx}{dt} = -\frac{\partial U}{\partial x} + \xi(t), \tag{3}$$

where

$$U(x) = -[A - S(t)]\frac{x^2}{2} + \frac{x^4}{4}, \tag{4}$$

A is a constant, $S(t)$ is an aperiodic (zero-mean) input signal, $\xi(t)$ is Gaussian white noise with zero mean and autocorrelation $\langle \xi(t)\xi(s)\rangle = 2D\delta(t-s)$, and the angular brackets denote an ensemble average. In this system, $S(t)$ modulates the barrier height and a disturbance is needed to switch the system's state point between the two wells. This disturbance is provided by $\xi(t)$, which acts as a thermal bath coupled to the system. For a given barrier height, a certain temperature (noise level) will allow the system's state point to overcome the barrier and switch wells. Thus, for a given noise level, the transition or hopping rate will be a function of the barrier height and hence a function of $S(t)$. This bistable-well system differs from the original bistable-well system of Ref. [2]: in the latter, the barrier height was alternately lowered for each of the wells, whereas in the former, the barrier height is lowered symmetrically for both wells.

To compute the power-norm measures [Eqs. (1) and (2)], we assume that the system's response $R(t)$ is characterized by the time-varying two-way transition or hopping rate [28]. In the numerical simulations, $R(t)$ was actually a mean transition rate formed by passing an averaging window over a train of impulses corresponding to the transition times. The numerical results [29] for the bistable-well system with an aperiodic input signal $S(t)$ are given in Fig. 1. (In the simulations, $A=1$.) Shown are the ensemble-averaged values (and standard errors) of C_0 and C_1 as a function of the input noise intensity D. (The solid curves are from the theory to be described below.) The results for C_1 [Fig. 1(b)] show characteristic signatures of ASR behavior: a rapid rise to a clear peak and then a slow decrease for higher values of noise intensity. The results for C_0 [Fig. 1(a)], on the other hand, increase monotonically with input noise intensity. The reason for this effect is described below.

We have developed a general theory for ASR. This theory requires an estimation of the mean first-passage time for a stochastically forced particle to pass over a barrier or reach a boundary. The mean first-passage time corresponds to the mean transition time of the system, from which the cross-correlation measures (i.e., C_0 and C_1) can be calculated. In the case of the bistable-well system, we use Kramers's classic result for the escape time of a particle over a potential barrier [30,31]. This then serves as an estimate of the mean transition rate between the wells. The Kramers rate is valid in the regime where the noise level is low compared to the barrier height. For large noise levels, the analysis breaks down and the notion of well hopping is better described as a boundary-crossing problem.

Using Kramers's formula, the ensemble-averaged rate of escape for a particle in a potential well is given by

$$\langle R(t)\rangle \simeq \frac{1}{2\pi}\sqrt{U''(x_{\min})|U''(x_{\max})|}\exp\left[\frac{U(x_{\min})-U(x_{\max})}{D}\right], \tag{5}$$

where $x_{\min}$ and $x_{\max}$ are the locations of one of the well minima and the maximum (barrier) for a potential function $U(x)$. (For a symmetric bistable-well system, the escape rate out of the other well is identical.)

To determine $x_{\min}$ and $x_{\max}$, we set [from Eq. (4)]

$$U'(x) = -[A - S(t)]x + x^3 = 0 \tag{6}$$

and solve to obtain the roots $x = 0, \pm[A-S(t)]^{1/2}$. This gives $x_{\min} = -[A-S(t)]^{1/2}$ and $x_{\max} = 0$. It can then be shown that

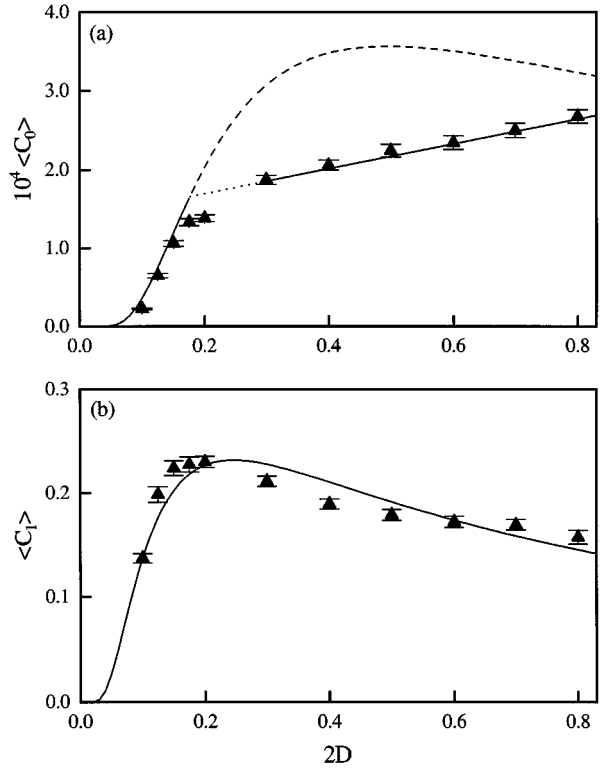

FIG. 1. Ensemble-averaged values (triangles) and standard errors of the (a) power norm C_0 and (b) normalized power norm C_1 versus $2D$, where D is the intensity of the input Gaussian white noise, for the bistable-well model with a weak aperiodic input signal $S(t)$. $S(t)$ was formed by convolving Gaussian correlated noise (with correlation time equal to 150 s) with a 100-s unit-area symmetric Hanning window filter. The same input signal $S(t)$, with variance equal to 2.14×10^{-3} and total time length equal to 3000 s, was used for all results presented. C_0 and C_1 were computed for each trial and then averaged over 700 trials using different seeds to generate the Gaussian white noise. The theoretical prediction for $\langle C_0 \rangle$ from Eq. (14) using the Kramers rate with $K_0=1$ is shown in (a) (solid and dashed curve). It is seen to match the data for small values of D, but breaks down for larger values of D where a linear curve (solid and dotted line) is shown to fit the data as expected from Eq. (20). The theoretical prediction for $\langle C_1 \rangle$ from Eq. (27) (solid curve) is shown in (b), with $K_1=0.019$.

$$U''(x_{\min})=2[A-S(t)], \tag{7}$$

$$U''(x_{\max})=-[A-S(t)], \tag{8}$$

$$U(x_{\min})=-[A-S(t)]^2/4, \tag{9}$$

$$U(x_{\max})=0. \tag{10}$$

Substituting these expressions into Eq. (5) yields

$$\langle R(t)\rangle \simeq \frac{\sqrt{2}}{2\pi}[A-S(t)]\exp\left[\frac{-[A-S(t)]^2}{4D}\right]. \tag{11}$$

Equation (11) is an estimate of the mean transition rate and a function of both the noise intensity D and the input signal $S(t)$. The power-norm measures are computed by cross-correlating this rate with $S(t)$ and averaging over time. $S(t)$ is independent of ensemble averaging so the ensemble-averaged power norm in Eq. (1) is

$$\langle C_0\rangle=\langle\overline{S(t)R(t)}\rangle\equiv\overline{S(t)\langle R(t)\rangle}. \tag{12}$$

To compute C_0, we use a time lag that corresponds to the peak in the input-output cross-correlation function [see Eq. (1)]. For notational simplicity, this time lag is suppressed but always implied.

In general, an explicit expression for the power norm does not exist. However, for the case where the signal amplitude is small compared to the barrier height, i.e., $\overline{S(t)^2}\ll A^2$, the rate can be expanded in a Taylor series in $S(t)$. We first expand the exponent in Eq. (11) and drop the $S(t)$ dependence in the amplitude to yield

$$\langle R(t)\rangle \simeq Q\exp[-\Theta+\Delta S(t)], \tag{13}$$

where $Q=K_0A/\sqrt{2}\pi$, $\Theta=A^2/4D$, and $\Delta=A/2D$. The parameter K_0 is included to account for normalization factors that may arise in the construction of the mean transition rate. The validity of these approximations will be discussed later.

Equation (13) can then be substituted into Eq. (12) to calculate $\langle C_0\rangle$. In the special case where $S(t)$ is a Gaussian-distributed signal, the time average can be performed explicitly to obtain the result

$$\langle C_0\rangle \simeq Q\Delta\exp[-\Theta+\Delta^2\overline{S^2(t)}/2]\overline{S^2(t)}. \tag{14}$$

For an arbitrary non-Gaussian signal, the rate Eq. (13) is expanded to first order in $S(t)$ to obtain

$$\langle C_0\rangle \simeq Q\Delta\exp[-\Theta]\overline{S^2(t)}. \tag{15}$$

This expression will be invalid for very small values of noise, namely, when $(A/4D)^2\overline{S^2(t)}\gtrsim 1$. However, for such noise levels, the rate will be very low and the errors will not be important. In the numerical simulations, we used a Gaussian noise source for $S(t)$, so to calculate C_0, we use Eq. (14). It should be noted that even this expression has already used a small-signal approximation and should be considered to be only slightly more accurate than the fully expanded form given by Eq. (15).

The expression for $\langle C_0\rangle$ given by Eq. (14) rises to a maximum value and then decreases with D. However, numerically, it was observed that $\langle C_0\rangle$ does not decay but continues to increase with D [Fig. 1(a)]. The reason for this discrepancy is that for larger noise levels, i.e., $D\gtrsim A^2/4$, the Kramers escape rate is no longer a good approximation for the transition rate. This is due to the fact that in the calculation of the escape rate, quasistationarity is assumed and for large D, this assumption is violated. To account for the behavior of the system in the large-D regime, we use a simple linear-ramp model for the well [32]. In this approximation, a straight line is drawn between $x_{\min}$ and $x_{\max}$. We then consider the first-passage time problem of a particle beginning at $x_{\min}$ and reaching $x_{\max}$. We shift the axis so that $x_{\min}=0$. Therefore, escape from the well reduces to

$$\dot{x}=-h+\xi(t), \tag{16}$$

where h is the slope of the ramp and $\xi(t)$ is zero-mean Gaussian white noise as in Eq. (3). Escape occurs at $x=L\equiv L_0+S(t)$. The first-passage time of such a problem is given by a converging infinite series [32]. Keeping only the first term, which should capture the essential qualitative picture, we have

$$t_0 \propto \frac{DF_1 k_1}{\lambda_1^2} \exp\left(\frac{-hL}{2D}\right), \tag{17}$$

where

$$F_1 = -\sinh k_1 L \left(\frac{L}{2} - \frac{\sinh 2k_1 L}{4k_1}\right)^{-1}, \tag{18}$$

$$\tan k_1 L = 2Dk_1/h, \quad \lambda_1 = \frac{h^2}{4D} + Dk_1^2. \tag{19}$$

For large D, $k_1 \sim \pi/(2L) - h/(\pi D)$ and F_1 saturates to a function of L. Thus $t_0 \propto D^{-1} F_1(L)/L$. The mean transition rate is given by $R(t)=1/t_0$, which increases with D, whereas the Kramers rate Eq. (13) saturates with increasing D. Expanding the rate in $S(t)$ and substituting into Eq. (12) yields

$$\langle C_0 \rangle \propto D\overline{S^2(t)}. \tag{20}$$

Hence $\langle C_0 \rangle$ continues to increase with D as observed in Fig. 1(a). This effect is not observed in excitable systems because of the saturating effect of the refractory time in such systems. This issue is discussed in greater detail in Sec. V.

The ensemble-averaged normalized power norm is given by

$$\langle C_1 \rangle \simeq \left\langle \frac{C_0}{N[\overline{S^2(t)}]^{1/2}} \right\rangle \simeq \frac{\langle C_0 \rangle}{N[\overline{S^2(t)}]^{1/2}}, \tag{21}$$

where

$$N^2 = \overline{[R(t) - \overline{R(t)}]^2}. \tag{22}$$

Previously, we made no distinction between the sample transition rate and the ensemble-averaged transition rate. However, in the calculation of N, we need to account for the time-dependent fluctuations in $R(t)$ due to the noise. Therefore, we use the ansatz that

$$R(t) \simeq \langle R(t) \rangle + \eta(t), \tag{23}$$

where $\langle R(t) \rangle$ is the Kramers escape rate [given by Eq. (13)] and $\eta(t)$ is a stochastic component that arises from the input noise, with $\overline{\eta(t)}=0$ and $\overline{\eta^2(t)} \equiv \sigma(D)$. [The stochastic component $\eta(t)$ does not affect the computation of $\langle C_0 \rangle$.]

Substituting Eq. (23) into Eq. (22) yields

$$N^2 = \overline{\langle R(t) \rangle^2} - \overline{\langle R(t) \rangle}^2 + \sigma(D). \tag{24}$$

Then, for the rate Eq. (13), where $S(t)$ is a Gaussian stochastic process,

$$\overline{\langle R(t) \rangle} \simeq Q \exp[-\Theta + \Delta^2 \overline{S^2(t)/2}] \tag{25}$$

and

$$\overline{\langle R(t) \rangle^2} \simeq Q^2 \exp[-2\Theta + 2\Delta^2 \overline{S^2(t)}]. \tag{26}$$

This then leads to an expression for $\langle C_1 \rangle$ [for $S(t)$ Gaussian]

$$\langle C_1 \rangle \simeq \frac{\Delta[\overline{S^2(t)}]^{1/2}}{\{\exp[\Delta^2 \overline{S^2(t)}] - 1 + \sigma(D) Q^{-2} \exp[2\Theta - \Delta^2 \overline{S^2(t)}]\}^{1/2}}. \tag{27}$$

The general case [for small $\overline{S^2(t)}$] is obtained by expanding to linear order in $\Delta^2 \overline{S^2(t)}$.

The noise-induced variance $\sigma(D)$ can be estimated by using an analogy to shot noise in electronics [33]. Consider the case where the signal $S(t)$ is zero. The occurrence of a transition from one well to the other is a random process and is analogous to the random arrival of an electron at a device. In this analogy, the mean transition rate corresponds to the current. For a pure Poisson process, the variance of the mean transition rate is proportional to the time average of the mean transition rate. In the present case, the hopping process will not be a pure Poisson process. However, we can use as an estimate for the variance

$$\sigma(D) = K_1 \overline{\langle R(t) \rangle}, \tag{28}$$

where K_1 is a constant. We can then insert Eq. (28) into Eq. (27).

The theoretical curves are plotted in Fig. 1. It can be seen in Fig. 1(a) that the expression for $\langle C_0 \rangle$ based on the Kramers rate [Eq. (14)] matches the data for small values of D but breaks down for larger values where $\langle C_0 \rangle$ behaves linearly, as predicted. The theoretical curve for $\langle C_1 \rangle$ [Eq. (27)] matches the data as seen in Fig. 1(b).

Finally, we mention that the theory predicts the shape of $\langle C_1 \rangle$ even when it is outside the range of its validity. This is an interesting circumstance. The theory is only properly valid for ranges of D near the peak location of $\langle C_1 \rangle$. For large values of noise, the Kramers rate no longer holds. However, in this regime, the stochastic contribution of $\sigma(D)$ dominates, so it does not matter so much that the Kramers rate is now a poor approximation. For very small values of D, the small $S(t)$ expansion breaks down, but the rate is so low that the errors are also suppressed.

IV. INTEGRATE-AND-FIRE NEURONAL MODEL

SR has been demonstrated in a variety of neuronal models [12,20–22,24,32,34–36], including integrate-and-fire models [22,32,36]. Here we consider an integrate-and-fire neuronal

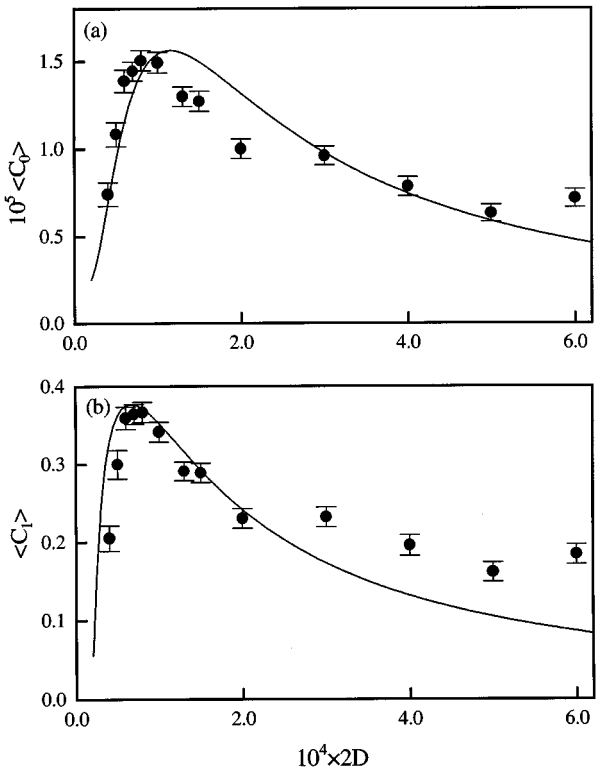

FIG. 2. Ensemble-averaged values (circles) and standard errors of the (a) power norm C_0 and (b) normalized power norm C_1 versus $2D$, where D is the intensity of the input Gaussian white noise, for the integrate-and-fire neuronal model with a subthreshold aperiodic input signal $S(t)$. $S(t)$ was formed by convolving Gaussian correlated noise (with correlation time equal to 150 s) with a 100-s unit-area symmetric Hanning window filter. The same input signal $S(t)$, with variance equal to 1.93×10^{-6} and total time length equal to 3000 s, was used for all results presented. C_0 and C_1 were computed for each trial and then averaged over 300 trials using different seeds to generate the Gaussian white noise. The theoretical predictions (solid curves) from Eqs. (32) and (34) are given in (a) and (b), respectively, with $K_0=0.22$ and $K_1=0.05$.

model with a subthreshold aperiodic input signal:

$$\dot{v} = -av + a - \delta + S(t) + \xi(t), \tag{29}$$

where v represents the voltage of the model neuron, a and δ are constants, δ/a is the barrier height, $S(t)$ is a subthreshold aperiodic input signal, and $\xi(t)$ is Gaussian white noise with zero mean and autocorrelation $\langle \xi(t)\xi(s)\rangle = 2D\delta(t-s)$. The firing threshold for this system is set at $v=1$.

To compute the power-norm measures, we assume that the system's response $R(t)$ is characterized by its time-varying mean firing rate. (This is a valid assumption for many types of sensory neurons [37].) In the numerical simulations, the time-varying mean firing rate was formed by passing a unit-area symmetric Hanning window filter over an impulse train corresponding to the firings of the model. The numerical results [29] for the integrate-and-fire neuronal model with a subthreshold aperiodic input signal are given in Fig. 2. (In the simulations, $a=0.5$ and $\delta=0.01$.) Shown are the ensemble-averaged values (and standard errors) of C_0 and C_1 as a function of the input noise intensity D. (The solid curves are from the theory to be described below.) The model exhibits clear ASR characteristics: $\langle C_0\rangle$ and $\langle C_1\rangle$, respectively, rapidly increase to a peak and then slowly decrease with increasing input noise intensity.

These numerical results can be understood analytically. We assume throughout that $\overline{S^2(t)} \ll \delta$. We first note that the average interpulse interval T is given by the first-passage distribution of the Ornstein-Uhlenbeck process Eq. (29). For the regime where $[\delta - S(t)]^2 \ll 2D$, a simple expression for T [38] is given by

$$\overline{T} \sim \frac{\sqrt{2D\pi}}{[\delta - S(t)]} \exp\left[\frac{[\delta - S(t)]^2}{2Da}\right]. \tag{30}$$

The ensemble-averaged mean firing rate is then given by

$$\langle R(t)\rangle \simeq \frac{\delta}{\sqrt{2D\pi}} \exp\left[\frac{-\delta^2 + 2\delta S(t)}{2Da}\right], \tag{31}$$

where we have employed a small $S(t)$ expansion.

The ensemble-averaged power norm is given by Eq. (12). Substituting Eq. (31) into Eq. (12) yields

$$\langle C_0\rangle \simeq Q\Delta \exp[-\Theta + \Delta^2 \overline{S^2(t)}/2]\overline{S^2(t)}, \tag{32}$$

where

$$Q = K_0\delta/\sqrt{2\pi D}, \quad \Theta = \delta^2/(2Da), \quad \Delta = \delta/(Da), \tag{33}$$

where K_0 is a free parameter. This form is for the case where $S(t)$ is a Gaussian-distributed signal. For a general signal, we can make an expansion in $S(t)$, as it was done with the bistable-well system in Sec. III.

The calculation of $\langle C_1\rangle$ is also similar to that for the bistable-well system. We use Eq. (27) directly, using Θ, Δ, and Q as defined in Eq. (33). We use the relation $\sigma(D) = K_1\langle \overline{R(t)}\rangle$, where $\langle R(t)\rangle$ is given by Eq. (31), to obtain

$$\langle C_1\rangle \simeq \frac{\Delta[\overline{S^2(t)}]^{1/2}}{\{\exp[\Delta^2\overline{S^2(t)}] - 1 + K_1 Q^{-1}\exp[\Theta - \Delta^2\overline{S^2(t)}/2]\}^{1/2}}. \tag{34}$$

Curves based on Eqs. (32) and (34) are shown in Fig. 2. The theory for $\langle C_0\rangle$ and $\langle C_1\rangle$, respectively, matches the data, predicting the location of the maximum. There is a deviation for larger values of D because the mean firing rate expression Eq. (31) begins to break down in that regime.

V. HODGKIN-HUXLEY NEURONAL MODEL

In our original ASR paper [14], we studied the dynamics of the FHN model because (i) it had been used in a number of physiologically motivated SR studies [12,20,24] and (ii) it provided a simple representation of the firing dynamics of sensory neurons. Here we consider the dynamics of a more sophisticated neuronal model [39], namely, the HH model [40]:

TABLE I. Parameter values used in the theory and simulations for the Hodgkin-Huxley neuronal model.

C	Membrane capacitance	1 μF/cm^2
v_L	Leakage reversal potential	-54.4 mV
g_L	Leakage conductance	0.3 mS/cm^2
v_K	Potassium reversal potential	-77 mV
$\overline{g_K}$	Maximal potassium conductance	36 mS/cm^2
ρ_K	Potassium ion-channel density	18 channels/μm^2
v_{Na}	Sodium reversal potential	50 mV
$\overline{g_{Na}}$	Maximal sodium conductance	120 mS/cm^2
ρ_{Na}	Sodium ion-channel density	60 channels/μm^2

$$C\dot{v} = -g_{Na}m^3h(v-v_{Na}) - g_K n^4(v-v_K) - g_L(v-v_L) + I + S(t) + \xi(t), \tag{35}$$

$$\dot{m} = \alpha_m(v)(1-m) - \beta_m(v)m, \tag{36}$$

$$\dot{h} = \alpha_h(v)(1-h) - \beta_h(v)h, \tag{37}$$

$$\dot{n} = \alpha_n(v)(1-n) - \beta_n(v)n, \tag{38}$$

where C is the capacitance; v is the membrane potential; the g's are constant conductances; v_{Na}, v_K, and v_L are constant equilibrium potentials; m, h, and n are variables representing sodium activation, sodium inactivation, and potassium activation channels, respectively; I is an input current; $S(t)$ is a subthreshold aperiodic input signal; $\xi(t)$ is zero-mean Gaussian white noise as in Eq. (3); and the α and β are rate constants. For our study, we use the classic Hodgkin-Huxley 6.3 °C values for the squid giant axon [40] shown in Table I. For these parameter values, the voltage-dependent rate constants have the form

$$\alpha_m = \frac{0.1(v+40)}{1-\exp[-(v+40)/10]}, \quad \beta_m = 4\exp[-(v+65)/18], \tag{39}$$

$$\alpha_h = 0.07\exp[-(v+65)/20],$$

$$\beta_h = \frac{1}{1+\exp[-(v+35)/10]}, \tag{40}$$

$$\alpha_n = \frac{0.01(v+55)}{1-\exp[-(v+55)/10]},$$

$$\beta_n = 0.125\exp[-(v+65)/80], \tag{41}$$

where v has units of mV and the rates have units of ms^{-1}.

As with the integrate-and-fire model (Sec. IV) and the FHN model [14], we assume that the HH model transmits information about input stimuli via temporal changes in its firing rate. We use this assumption to compute the power-norm measures. (In the numerical simulations, the time-varying mean firing rate for the HH model was formed by passing a unit-area symmetric Hanning window filter over an impulse train corresponding to the firings of the model.) The numerical results [29] for the HH model with a subthreshold aperiodic input signal $S(t)$ are given in Fig. 3. (In the simulations, $I=0$.) Shown are the ensemble-averaged values (and standard errors) of C_0 and C_1 as a function of the input noise intensity D. (The solid curves are from the theory to be described below.) As with the integrate-and-fire model (Fig. 2) and the FHN model [14], the HH model exhibits clear ASR characteristics: the respective power-norm measures rapidly increase to a peak and then slowly decrease with increasing input noise intensity.

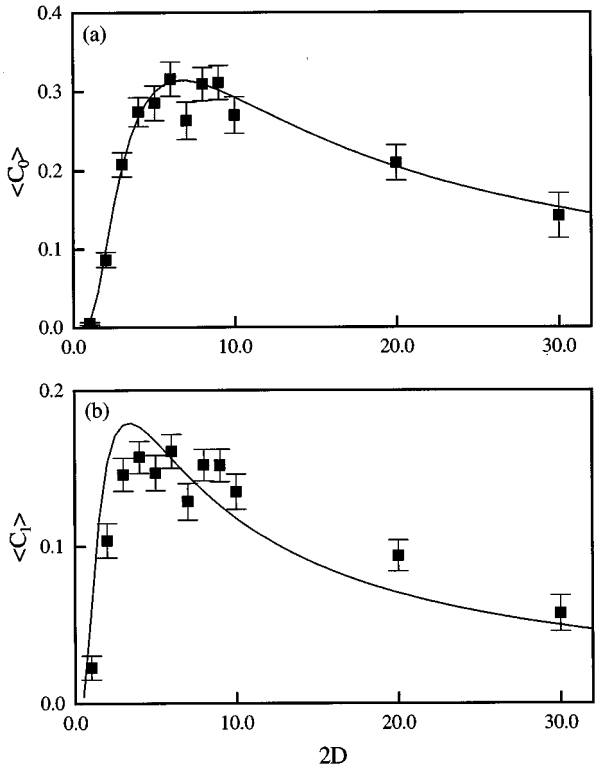

FIG. 3. Ensemble-averaged values (squares) and standard errors of the (a) power norm C_0 and (b) normalized power norm C_1 versus $2D$, where D is the intensity of the input Gaussian white noise, for the Hodgkin-Huxley neuronal model with a subthreshold aperiodic input signal $S(t)$. $S(t)$ was formed by convolving Gaussian correlated noise (with correlation time equal to 0.25 s) with a 0.25-s unit-area symmetric Hanning window filter. The same input signal $S(t)$, with variance equal to 1.23×10^{-1} and total time length equal to 10 s, was used for all results presented. C_0 and C_1 were computed for each trial and then averaged over 200 trials using different seeds to generate the Gaussian white noise. The theoretical predictions (solid curves) based on Eqs. (32) and (34) are given in (a) and (b), respectively, using $Q=K_0(0.045+0.12\epsilon)$, $\Theta=(0.32+2.76\epsilon)/D$, and $\Delta=0.24/D$, with $K_0=0.55$, $K_1=1$, and $\epsilon=1.1$ mV.

Below we develop a general theory for ASR in excitable membranes. This theory will be applicable to both the HH model and the FHN model, as well as other excitable-membrane models. An excitable membrane with stochastic forcing will generally have the form [41]

$$C\dot{v} = I_{\text{ion}}(v,\{w_i(v)\}) + I(t) + \xi(t), \tag{42}$$

where v is the membrane potential, $\{w_i(v)\}$ are the fraction of open channels for a set of n ion-channel types, $I(t)$ is input current, and $\xi(t)$ is zero-mean Gaussian white noise. The $w_i(v)$ channels obey equations of the form

$$\dot{w}_i = \alpha_i(v)(1-w_i) - \beta_i(v) w_i, \tag{43}$$

where $\alpha_i(v)$ and $\beta_i(v)$ are rate constants. Each w_i channel has an asymptotic value of $w_{i,\infty}(v) = \alpha_i(v)/[\alpha_i(v)+\beta_i(v)]$ and a characteristic time scale of $\tau_i(v) = [\alpha_i(v) + \beta_i(v)]^{-1}$. To compute C_0 and C_1 as functions of D, we need to obtain the mean firing rate due to a subthreshold input signal plus noise. This is done by transforming Eq. (42) into a ''double-well'' Langevin equation, where the Kramers escape rate from one minimum to the other can be used for the mean firing rate.

For a subthreshold input signal, the voltage is at a stable resting point $v = v_R$. Consider a subthreshold input signal of the form $I(t) = I_0 + S(t)$, where I_0 is a dc signal and $S(t)$ is an arbitrary zero-mean time-varying signal that is slow and small in amplitude. (The meaning of slow and small will be defined later.) The resting voltage is found by setting [from Eq. (42)]

$$\dot{v} = \dot{w}_i = 0. \tag{44}$$

Assume that

$$v_r(t) = \overline{v_r} + aS(t), \tag{45}$$

where $\overline{v_r}$ can be found numerically or analytically by setting $S(t) = 0$ in Eq. (44). The parameter a can be found by substituting Eq. (45) into Eq. (44) [with $S(t)$ intact] and solving to first order in $S(t)$.

In general, Eq. (42) contains a wide range of time scales. If all the channels are either fast or slow, then Eq. (42) can be simplified to a first-order Langevin equation. If there is not a separation of time scales, a multidimensional problem must be studied. In the HH model studied here, there is only a partial separation of time scales and thus the theory is not directly applicable in the present format. However, as will be shown, it can be modified to account for this lack of full separation.

The approximation we use is to let all fast channels be instantaneous and all slow channels be fixed near rest. This assumption works because we are only concerned with the generation of action potentials from a resting state. Once an action potential is generated, the slow variables play a role in restoring the membrane potential (i.e., voltage) to rest [42]. Therefore, we divide $I_{\rm ion}$ into fast and slow currents

$$I_{\rm ion} = I_f(v, \{w_f\}) + I_s(v, \{w_s\}), \tag{46}$$

where $\{w_f\}$ and $\{w_s\}$ are the sets of fast and slow channels, respectively. The fast channels are taken to be instantaneous, i.e., $w_f = w_{f,\infty}(v)$, and we fix the slow channels to the resting value

$$w_s = w_{s,\infty}(v = v_R). \tag{47}$$

With these assumptions, Eq. (42) becomes

$$C\dot{v} = I_f(v, \{w_{f,\infty}(v)\}) + I_s(v, \{w_{s,\infty}(v_R)\}) + I_0 + S(t) + \xi(t), \tag{48}$$

which can be rewritten as

$$C\dot{v} = u(v, S(t)) + \xi(t), \tag{49}$$

where $u = -U'(v)$. For a subthreshold input signal $I(t)$, $U(v)$ is a double-well (bistable) potential, with minima at v_1 and v_3 and a maximum at v_2. (Note that $v_1 \equiv v_R$.) Action potentials occur when v jumps from near v_1 to v_3 over the barrier at v_2. We know $v_1(S) = v_r = \overline{v_r} + aS(t)$. We find v_2 and v_3 by solving $u(v,S) = 0$, although it is not necessary to find v_3 for this calculation.

The ensemble-averaged mean firing rate $\langle R(t) \rangle$ for the system is given by the Kramers rate

$$\langle R(t) \rangle \simeq \frac{1}{2\pi C} \sqrt{U''(v_1)|U''(v_2)|} \exp[CU_0/D], \tag{50}$$

where $U_0 \equiv U(v_1) - U(v_2)$. The rate $\langle R(t) \rangle$ is a function of $S(t)$, and this dependence must be made explicit. We reexpress U_0 as

$$U_0(S) = \int_{v_1(S)}^{v_2(S)} u(v'; S)\, dv'. \tag{51}$$

Expanding for small $S(t)$, it can be shown that

$$U_0(S) = \int_{v_1(0)}^{v_2(0)} u(v'; 0)\, dv' + \left[\int_{v_1(0)}^{v_2(0)} \partial_S u(v'; 0)\, dv' \right] S(t), \tag{52}$$

where we have used the fact that $u(v_1, 0) = u(v_2, 0) = 0$. In addition,

$$U''(v_1) = -u'(v_1), \tag{53}$$

$$U''(v_2) = -u'(v_2), \tag{54}$$

where the prime refers to derivative with respect to v. The ensemble-averaged mean firing rate is then given by

$$\langle R(t) \rangle \simeq \frac{1}{2\pi C} \sqrt{|u'(v_1)| u'(v_2)} \exp[CU_0(S)/D], \tag{55}$$

where $U_0(S)$ is given by Eq. (52).

We first apply this formulation to the FHN model, which we write in the form [14]

$$C\dot{v} = -v(v^2 - \tfrac{1}{4}) - w + A_T - \gamma + \xi(t), \tag{56}$$

$$\dot{w} = v - w, \tag{57}$$

where $v(t)$ is a voltage variable, $w(t)$ is a recovery variable, $A_T = -5/(12\sqrt{3})$ is a threshold voltage, $\gamma = B - S(t)$, B is a constant parameter corresponding to the signal-to-threshold distance, $S(t)$ is the input signal, and $\xi(t)$ is the standard noise source. In the FHN model, the fast channel is modeled by the nonlinear term in Eq. (56) and is already taken to be instantaneous. The slow channel is given by Eq. (57). The fixed point of the system, obtained by setting $\dot{v} = \dot{w} = 0$, is approximately given by $v_r \simeq -1/(2\sqrt{3}) - \gamma + (\sqrt{3}/2)\gamma^2$. The time scales of the two variables can be estimated by linearizing around the resting value. We find that w has a characteristic time of $\tau_w \sim 1$ and v has a time of $\tau_v \sim 6C/5$. Thus, for C very small, v is a much faster variable than w.

We then set the slow channel to its resting value (given by $w \simeq v_r$) to obtain the one-dimensional Langevin equation

$$C\dot{v} \simeq u(v) + \xi(t), \tag{58}$$

where

$$u(v) \equiv -U'(v) = -(A - v/4 + v^3), \tag{59}$$

$$A = -1/(12\sqrt{3}) + \sqrt{3}/2\gamma^2. \tag{60}$$

The potential $U(v)$ is a double well with one minimum at $v_1 = v_r$ and a maximum at $v_2 \simeq -1/(2\sqrt{3}) + \gamma$. Applying Eq. (55) yields

$$\langle R(t) \rangle \propto \frac{B}{2\pi\sqrt{3}C} \exp\left[\frac{-2\sqrt{3}C[B^3 - 3B^2 S(t)]}{3D}\right]. \tag{61}$$

(This result differs slightly from the result in Ref. [14].) The cross-correlation measures $\langle C_0 \rangle$ and $\langle C_1 \rangle$ are then computed as in Ref. [14] and Sec. III. It should be noted that the problem of increasing firing rate (and hence $\langle C_0 \rangle$) in the large-D regime is not encountered in the FHN model [14]. The reason for this is that the FHN model and other excitable systems have an associated refractory or dead time. Thus, after a firing event has occurred, there is a finite amount of time before another one can occur. This refractory time imposes a saturation mechanism onto the firing rate.

We now apply the formalism to the HH model. We use the parameters of Table I with $I = 0$. The resting potential of the HH model for $S(t) = 0$ can be found numerically with the result $\overline{v_r} = -65$ mV. Setting $v_r = \overline{v_r} + aS(t)$ and substituting this into Eq. (44) [with $S(t)$ intact] gives the value $a = 0.86$. Near resting potential, the characteristic time scales are $\tau_v \sim 1.4$ ms, $\tau_m \sim 0.24$ ms, $\tau_h \sim 8.3$ ms, and $\tau_n \sim 5.6$ ms. The m channel is faster than the potential v and the h and n channels are slower. However, there is not a vast separation of time scales as in the FHN model. ($C = 0.005$ was used in the numerical simulations for the FHN model [14].) Employing the formalism, we would let the m channel be instantaneous and freeze the h and n channels to their resting values. The effective Langevin equation would be given by

$$C\dot{v} \simeq u(v, S(t)) + \xi(t), \tag{62}$$

where

$$u(v, S(t)) = -g_{Na} m_\infty^3(v) h_\infty(v_r)(v - v_{Na}) - g_K n_\infty^4(v_r)(v - v_K) - g_L(v - v_L) + S(t). \tag{63}$$

However, because there is not a large separation of time scales, the h and n channels will tend to drift in response to fluctuations in v. We note that h and n are ''restoring'' variables that will tend to increase the effective barrier. We can account for this by ''shifting the path'' of the effective Langevin equation to take into account the dynamics of the slow channels. We do this by moving the resting values of n and h. We perturb the resting value by a small amount $v_r = \overline{v_r} + \epsilon$. We then substitute this into Eq. (63) and expand to linear order so that

$$u(v, S(t), \epsilon) = u(v, S(t), 0) + \partial_\epsilon u(v, S(t), 0)\epsilon. \tag{64}$$

Both v_1 and v_2 will shift: $v_j = \overline{v_j} - [\partial_\epsilon u(\overline{v_j}, 0, 0)/u'(\overline{v_j}, 0, 0)]\epsilon$, for $j = 1, 2$, where $\overline{v_j}$ is the root of $u(v, 0, 0) = 0$. This results in

$$U_0(S) \simeq \int_{\overline{v_1}}^{\overline{v_2}} [u(v', 0, 0) + \partial_\epsilon u(v, 0, 0)]\, dv' + \left[\int_{\overline{v_1}}^{\overline{v_2}} [\partial_S u(v', 0, 0)]\, dv'\right] S(t), \tag{65}$$

$$u'(v_j, \epsilon, 0) = u'(\overline{v_j}, 0, 0) + [u''(\overline{v_j}, 0, 0) \times [\partial_\epsilon u(\overline{v_j}, 0, 0)/u'(\overline{v_j}, 0, 0)] + \partial_\epsilon u'(\overline{v_j}, 0, 0)]\epsilon. \tag{66}$$

Solving $u(v, 0, 0) = 0$ yields $\overline{v_1} = \overline{v_r}$, $\overline{v_2} = -62.38$ mV. We insert Eq. (64) into Eq. (52), keep terms to linear order in ϵ and $S(t)$, perform the definite integrals numerically, and obtain

$$U_0 = -0.32 - 2.76\epsilon + 0.24 S(t), \tag{67}$$

$$u'(v_1) = -0.25 - 0.53\epsilon, \tag{68}$$

$$u'(v_2) = 0.32 + 1.05\epsilon. \tag{69}$$

Substituting these results into Eq. (55) gives

$$\langle R(t) \rangle = (0.045 + 0.12\epsilon) \exp\{[-0.32 - 2.76\epsilon + 0.24 S(t)]/D\} \ \text{ms}^{-1}. \tag{70}$$

This rate can now be used in Eq. (32) for $\langle C_0 \rangle$ and Eq. (34) for $\langle C_1 \rangle$, using $Q = K_0(0.045 + 0.12\epsilon)$, $\Theta = (0.32 + 2.76\epsilon)/D$, and $\Delta = 0.24/D$. Curves based on Eqs. (32) and (34) are shown in Fig. 3. The rates in the simulations were expressed in units of s^{-1}. The calculated rate can be converted to these units by multiplying Q by a factor of 1000. The theory for $\langle C_0 \rangle$ and $\langle C_1 \rangle$, respectively, matches the data, predicting the location of the maximum.

VI. CONCLUSIONS AND IMPLICATIONS

This work clearly shows that SR-type behavior is not limited to systems with periodic inputs. Thus, in general, noise can serve to enhance the response of a nonlinear system to a weak input signal, regardless of whether the signal is periodic or aperiodic. These developments suggest that SR-type dynamics could be exploited in systems with broadband input signals. This could be particularly useful for the design of signal-detection devices, such as superconducting quantum interference devices [6,43]. This work also lends further

support to the notion [14,16] that it may be possible to develop ASR-based bioengineering techniques for improving the function of neurophysiological sensory systems, such as the somatosensory system. With such techniques, noise could be introduced artificially into sensory neurons in order to improve their abilities to detect arbitrary weak signals. Techniques of this sort could be used to improve sensory function in healthy individuals and individuals with sensory thresholds that are elevated due to disease or normal aging.

ACKNOWLEDGMENT

This work was supported by the National Science Foundation.

[1] F. Moss, D. Pierson, and D. O'Gorman, Int. J. Bifurc. Chaos **4**, 1383 (1994); K. Wiesenfeld and F. Moss, Nature **373**, 33 (1995); A.R. Bulsara and L. Gammaitoni, Phys. Today **49**(3), 39 (1996).

[2] R. Benzi, S. Sutera, and A. Vulpiani, J. Phys. A **14**, L453 (1981); C. Nicolis, Tellus **34**, 1 (1982); R. Benzi, G. Parisi, A. Sutera, and A. Vulpiani, *ibid.* **34**, 11 (1982).

[3] S. Fauve and F. Heslot, Phys. Lett. **97A**, 5 (1983); R.N. Mantegna and B. Spagnolo, Phys. Rev. E **49**, R1792 (1994).

[4] B. McNamara, K. Wiesenfeld, and R. Roy, Phys. Rev. Lett. **60**, 2626 (1988); J. Grohs, S. Apanasevich, P. Jung, H. Ißler, D. Burak, and C. Klingshirn, Phys. Rev. A **49**, 2199 (1994); J.M. Iannelli, A. Yariv, T.R. Chen, and Y.H. Zhuang, Appl. Phys. Lett. **65**, 1983 (1994); J.P. Sharpe, N. Sungar, and N. Macaria, Opt. Commun. **114**, 25 (1995); M.I. Dykman, G.P. Golubev, I.Kh. Kaufman, D.G. Luchinsky, P.V.E. McClintock, and E.A. Zhukov, Appl. Phys. Lett. **67**, 308 (1995); B.M. Jost and B.E.A. Saleh, Opt. Lett. **21**, 287 (1996).

[5] L. Gammaitoni, M. Martinelli, L. Pardi, and S. Santucci, Phys. Rev. Lett. **67**, 1799 (1991).

[6] A.D. Hibbs, A.L. Singsaas, E.W. Jacobs, A.R. Bulsara, J.J. Bekkedahl, and F. Moss, J. Appl. Phys. **77**, 2582 (1995).

[7] M.L. Spano, M. Wun-Fogle, and W.L. Ditto, Phys. Rev. A **46**, 5353 (1992).

[8] A. Longtin, A. Bulsara, and F. Moss, Phys. Rev. Lett. **67**, 656 (1991).

[9] J.K. Douglass, L. Wilkens, E. Pantazelou, and F. Moss, Nature **365**, 337 (1993).

[10] S.M. Bezrukov and I. Vodyanoy, Nature **378**, 362 (1995).

[11] B. McNamara and K. Wiesenfeld, Phys. Rev. A **39**, 4854 (1989); L. Gammaitoni, F. Marchesoni, E. Menichella-Saetta, and S. Santucci, Phys. Rev. Lett. **62**, 349 (1989); P. Jung and P. Hänggi, Europhys. Lett. **8**, 505 (1989); P. Jung, Phys. Rep. **234**, 175 (1993); M.I. Dykman *et al.*, Phys. Lett. A **180**, 332 (1993); V.A. Shneidman, P. Jung, and P. Hänggi, Phys. Rev. Lett. **72**, 2682 (1994).

[12] K. Wiesenfeld, D. Pierson, E. Pantazelou, C. Dames, and F. Moss, Phys. Rev. Lett. **72**, 2125 (1994).

[13] P. Jung, Phys. Rev. E **50**, 2513 (1994); Phys. Lett. A **207**, 93 (1995); Z. Gingl, L.B. Kiss, and F. Moss, Europhys. Lett. **29**, 191 (1995); L. Gammaitoni, Phys. Rev. E **52**, 4691 (1995); Phys. Lett. A **208**, 315 (1995).

[14] J.J. Collins, C.C. Chow, and T.T. Imhoff, Phys. Rev. E **52**, R3321 (1995).

[15] J.J. Collins, C.C. Chow, and T.T. Imhoff, Nature **376**, 236 (1995).

[16] J.J. Collins, T.T. Imhoff, and P. Grigg, J. Neurophysiol. **76**, 642 (1996).

[17] Kiss independently developed a theory for SR-type behavior in threshold devices with wideband input signals [L.B. Kiss, in *Proceedings of the Third Technical Conference on Nonlinear Dynamics (Chaos) and Full Spectrum Processing*, edited by R. Katz (AIP, New York, in press)].

[18] P. Jung and P. Hänggi, Phys. Rev. A **44**, 8032 (1991).

[19] A. Neiman and L. Schimansky-Geier, Phys. Rev. Lett. **72**, 2988 (1994).

[20] F. Moss, J.K. Douglass, L. Wilkens, D. Pierson, and E. Pantazelou, Ann. N.Y. Acad. Sci. **706**, 26 (1993).

[21] A. Bulsara, E.W. Jacobs, T. Zhou, F. Moss, and L. Kiss, J. Theor. Biol. **152**, 531 (1991).

[22] A.R. Bulsara, S.B. Lowen, and C.D. Rees, Phys. Rev. E **49**, 4989 (1994).

[23] This technique is based on the concept of residence-time probability density functions [T. Zhou, F. Moss, and P. Jung, Phys. Rev. A **42**, 3161 (1990)].

[24] A.J. Longtin, J. Stat. Phys. **70**, 309 (1993).

[25] A. Zador and A.R. Bulsara, Phys. Rev. E **54**, R2185 (1996); M. Stemmler (unpublished).

[26] C. Heneghan, C.C. Chow, J.J. Collins, T.T. Imhoff, S.B. Lowen, and M.C. Teich, Phys. Rev. E **54**, R2228 (1996).

[27] J.E. Levin and J.P. Miller, Nature **380**, 165 (1996).

[28] The time-varying two-way hopping rate was computed by passing a unit-area symmetric Hanning window filter over an impulse train corresponding to the well transitions in the system. (An impulse was recorded every time the system's state point crossed $x=0$.)

[29] The model equations were solved numerically using an algorithm developed for stochastic differential equations [R. Mannella and V. Palleschi, Phys. Rev. A **40**, 3381 (1989)]. An integration step size of 0.01 s, 0.1 s, and 0.05 ms was used for the bistable-well, integrate-and-fire, and Hodgkin-Huxley models, respectively. The reported results did not change for smaller stepsizes.

[30] H.A. Kramers, Physica **7**, 284 (1940).

[31] For an excellent review of work on Kramers's rate theory, see P. Hänggi, P. Talkner, and M. Borkovec, Rev. Mod. Phys. **62**, 251 (1990).

[32] A.R. Bulsara, T.C. Elston, C.R. Doering, S.B. Lowen, and K. Lindenberg, Phys. Rev. E **53**, 3958 (1996).

[33] S.O. Rice, in *Selected Papers on Noise and Stochastic Processes*, edited by N. Wax (Dover, New York, 1954).

[34] D.R. Chialvo and A.V. Apkarian, J. Stat. Phys. **70**, 375 (1993).

[35] M. Stemmler, M. Usher, and E. Niebur, Science **269**, 1877 (1995).

[36] F. Chapeau-Blondeau, X. Godivier, and N. Chambet, Phys. Rev. E **53**, 1273 (1996).

[37] G.M. Shepherd, *Neurobiology*, 2nd ed. (Oxford University Press, Oxford, 1988).

[38] H.C. Tuckwell, *Stochastic Processes in the Neurosciences* (SIAM, Philadelphia, 1989).

[39] The FHN model was originally proposed as a simplified version of the HH model [R.A. FitzHugh, Biophys. J. **1**, 445 (1961); J. Nagumo, S. Arimoto, and S. Yoshizawa, Proc. IRE **50**, 2061 (1962)].

[40] A.L. Hodgkin and A.F. Huxley, J. Physiol. **117**, 500 (1952).

[41] J. Rinzel and G.B. Ermentrout, in *Methods in Neuronal Modelling*, edited by C. Koch and I. Segev (MIT Press, Cambridge, 1989).

[42] Some excitable-membrane models, like the HH model, have fast deactivating channels. These channels, however, are slow near rest and deactivate when the voltage increases during the generation of an action potential.

[43] R. Rouse, S. Han, and J.E. Lukens, Appl. Phys. Lett. **66**, 108 (1995).